JOURNAL OF APPLIED ELECTROCHEMISTRY **23** (1993) 1017–1024

Effect of impurities on the corrosion behaviour of neodymium

H. BALA*, S. SZYMURA‡, G. PAWŁOWSKA*

Department of Chemistry and Institute of Physics‡, Polytechnic of Czestochowa, Al.Armii Krajowej 19,*
PL 42-200 Czestochowa, Poland

YU. M. RABINOVICH

Research and Technology Enterprise MIRT, Gospitalnyi Val 5-18 kv.172 105094 Moscow, Russia

Received 13 April 1992; revised 2 February 1993

The corrosion behaviour of neodymium contaminated with up to 0.9% C, up to 15% Fe and about 16% of Tb or Dy was examined in various aggressive environments. It was found that in acid media the C and Fe additions accelerated the corrosion process of the alloys. The Nd-base alloys were fairly resistant to corrosion in atmospheric conditions, however, the impurities worsened the corrosion behaviour in this environment as compared with pure Nd.

1. Introduction

In the early 1980s wide application of new high-performance RE–Fe–B type magnets (where RE = Nd, more rarely Pr or Dy or their compositions) began in many countries. The magnets exhibit excellent magnetic properties, however, they suffer strongly from great sensitivity to corrosion in many aggressive environments. This poor resistance to corrosion results from the presence of relatively high amounts of rare earth elements (30–35 wt %). The rare earth elements are among the most electrochemically active metals, the standard potentials for RE/RE^{3+} systems being −2.6 to −2.0 V [1].

The corrosion mechanism of Nd–Fe–B type magnets consists of the preferential oxidation (dissolution) of a Nd-rich phase (chemical formula Nd_4Fe), situated between the grains of a ferromagnetic $Nd_2Fe_{14}B$ phase. This causes surface degradation, a worsening of magnetic properties, and sometimes reduces to pulverization. The corrosion mechanism of RE-containing permanent magnets is discussed in [2–6]. The susceptibility of the Nd-rich phase to corrosion can be reduced by such alloying additions as Co (about 5 at %) [4, 7] or 1 at % of Cr, Al, Ti and Zr [6, 7]; these additions also improve the magnetic properties of the alloys.

In permanent magnet technology a high grade purity neodymium is used, which increases the price of the magnet [8]. The separation and purification of RE elements is a complex process. Especially undesirable impurities of RE elements are considered to be mainly O and C [9] because these impurities degrade the coercive force of the RE–Fe–B magnets. On the other hand, the presence of decimal percentages of carbon in the alloy causes a strong enrichment of the Nd-rich phase (during sintering inclusions of NdC_2 carbide appear [9]), which can have significant consequences for the corrosion behaviour.

Taking into account that the corrosion resistance of sintered Nd–Fe–B type magnets is determined mainly by the electrochemical activity of the Nd-rich phase (containing 75–85 wt % Nd), it is important to know the effect of technological impurities on the corrosion behaviour of RE alloys.

There is little literature concerned with the problem of corrosion behaviour of pure RE metals and their alloys. In [10, 11] the corrosion characteristics of pure (99.9%) RE metals (apart from Pm) are presented, however, they refer mainly to the metal's behaviour in atmospheric conditions and at elevated temperatures. Rybakov *et al.* [12, 13] noticed the important role of air pollutants (SO_2, H_2O, CO_2) on the corrosion of pure metals: La (99.9%) and Ce (99.8%). All cited authors believe that the corrosiveness of air rises sharply with an increase in relative humidity. Lee and Greene [11] consider RE-oxides to have protective properties whereas hydroxides (formed on the surface in the presence of humidity in the air) do not protect the surface of the RE-metal against further corrosion attack.

To characterize the corrosion behaviour of RE metals in acid media, it is important to consider the possibility of the creation of RE hydrides as products of the corrosion process. The great affinity of RE metals to hydrogen is commonly known. Gaseous hydrogen reacts with RE elements at room temperature. In the case of Nd–Fe–B magnets, the creation of hydrides in both the ferromagnetic and Nd-rich phases was found. As a result, non-stoichiometric products, with formulae $Nd_2Fe_{14}BH_{3.3}$ and $NdH_{2.8}$, respectively, are formed [14]. Absorption of gaseous

0021-891X

*Table 1. Chemical composition (wt %) of the tested alloys of neodymium**

No.	*Type*	*Notation*	*Nd*	*Sum of Ln*†			*C*	*Fe*	*O*
				Tb	*Dy*	*other Ln*			
1	(i)	Nd–0.6Fe	97.3		1.3		0.10	0.56	0.6
2		Nd–8.3Fe	89.8		1.1		0.10	8.3	0.7
3		Nd–15 Fe	83.0		1.0		0.10	15.0	0.8
4	(ii)	Nd–Fe	83.0	0.1	0.1	0.8	0.10	15.0	0.8
5		Nd(Tb)–Fe	68.0	15.6	0.2	1.7	0.10	14.0	0.7
6		Nd(Dy)–Fe	67.5	0.3	16.9	1.6	0.10	13.0	0.7
7	(iii)	Nd–0.1C	97.3		1.3		0.10	0.5	0.6
8		Nd–0.3C	97.5		1.2		0.26	0.1	0.6
9		Nd–0.9C	96.9		1.4		0.86	0.1	0.6
10		pure Nd	99.5		~0.3		<0.1	<0.1	<0.1

*Apart from elements specified in the Table, the tested alloys contained 0.06–0.12% Ca and 0.04–0.1% Cl.
†Ln = lanthanides, mainly Pr.

hydrogen by Nd–Fe–B alloys, and as a result, the so called decrepitation of the material is today considered as a promising method of the Nd–Fe–B powder preparation just before sintering [15].

The present work aims at the gravimetric and electrochemical evaluation of the corrosion resistance of three kinds of neodymium alloys: Nd–Fe, Nd(Ln)–Fe and Nd–C with the intention of considering their possible application in permanent magnet production.

2. Experimental details

Three kinds of Nd-base alloys were investigated:
(i) Nd–Fe alloys, containing 0.6–15 wt % Fe;
(ii) Nd(Ln)–Fe alloys, in which neodymium was partly substituted by 16–17 wt % of other lanthanides (Tb and Dy) and 13–15 wt % Fe;
(iii) Nd–C alloys, containing 0.1–0.9 wt % C.
For comparative purposes pure neodymium (~99.5 wt %) was used. The chemical composition of the tested samples are presented in Table 1.

The corrosion behaviour of the tested Nd-base alloys was studied in two acid sulphate solutions (pH 0.3 and 3.0) and in a so called 'industrial atmosphere' by gravimetric and polarization methods. The following corrosion tests were carried out:
(a) Acid corrosion test: spontaneous dissolution of the samples in deaerated, argon saturated 0.5 M H_2SO_4 solution at 25° C, without stirring.
(b) Accelerated test on atmospheric corrosion: long-lasting exposure of the tested samples in humidity saturated air containing 3 mg dm^{-3} SO_2 at 40° C.
(c) Potentiokinetic polarization curves: argon saturated solution of acidified (pH 3) 0.5 M Na_2SO_4 (25° C), disc electrode rotation speed 12 r.p.s., potential scanning rate 200 mV min^{-1} starting at potential –2.0 V up to –0.5 V vs SCE (saturated calomel electrode).
Samples for gravimetric tests (a) and (b) had the form of rectangular plates with an operating surface are a $S = 10\,\mathrm{cm}^2$. Samples for the potentiokinetic measurements (c) had the shape of rotating discs with $S = 0.1\,\mathrm{cm}^2$. Details of the apparatus and test methods are given in [5–7].

3. Results and discussion

3.1. *Acid corrosion test*

For the most part, mass losses of the tested Nd-base alloys increase linearly with time of exposure in the 0.5 M sulphuric acid solution (corrosion rate constant with time). Only for samples Nd–0.3C and Nd–0.9C did the corrosion rate initially decrease a little then settle to a constant level after 1–2 min of etching. In Fig. 1, as an example, corresponding relationships $(\Delta mS^{-1}) = f(\tau)$ for two Nd–Fe alloys are presented. From the slope of the straight lines the values of corrosion rate can be calculated. For the alloys Nd–0.6Fe and Nd–8.3Fe these values are 3480 ± 180 and $2550 \pm 100\,\mathrm{mg\,cm^{-2}\,h^{-1}}$, respectively. Analogously determined acid corrosion rates for the rest of the tested alloys are presented in Table 2. As shown in Table 2, an increase in Fe content in neodymium causes a decrease in the corrosion rate. A similar effect will probably be caused by any other

Table 2. Spontaneous dissolution rates of the tested Nd-base alloys in 0.5 M sulphuric acid solution (Ar, 25° C)

No.	*Alloy notation*	V_{corr}/mg cm^{-2}h^{-1}	Error/%
1	Nd–0.6Fe	3480	± 5.2
2	Nd–8.3Fe	2550	± 3.7
3	Nd–15 Fe	2470	± 4.1
4	Nd–Fe	2470	± 4.1
5	Nd(Tb)–Fe	2420	± 4.0
6	Nd(Dy)–Fe	2370	± 3.0
7	Nd–0.1C	3480	± 5.2
8	Nd–0.3C	3150*	± 5.0
9	Nd–0.9C	2820*	±4.7
10	pure Nd	1510	± 2.0

*In steady-state conditions (after 1–2 min of etching).

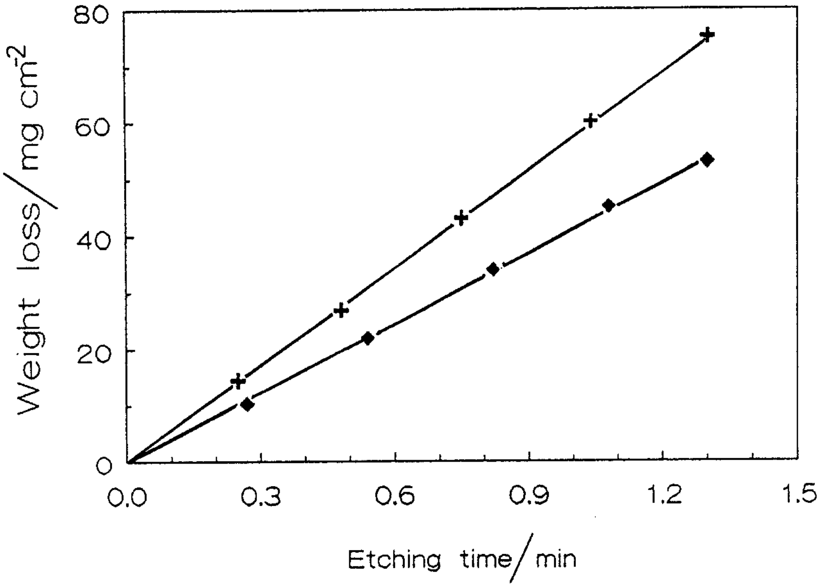

Fig. 1. Results of spontaneous dissolution of two Nd–Fe alloys in deaerated, non-stirred 0.5 M H_2SO_4 solution at 25° C. (+) Nd–0.6%Fe; (◆) Nd–8.3%Fe.

additions of more noble (as compared with Nd) metals. From the literature, it is known that the enrichment of the Nd-rich phase with Co is especially advantageous for protection of Nd–Fe–B type magnets against corrosion [4, 16]. Partial substitution of Nd with another lanthanide (Tb or Dy) has practically no influence on the acid corrosion behaviour of the alloy, whereas C additions distinctly inhibit the corrosion process. It should be noted that the initial corrosion rates of all the tested Nd–C alloys were close to each other. Differences between particular samples appear after 1–2 min of exposure, when the corroding surface of alloys containing 0.3 and 0.9% C becomes covered with a black slime of graphite. This layer of slime is responsible for the inhibition of the acid corrosion process.

All the tested Nd base alloys exhibited greater corrosion rates in the acid solution than pure neodymium which points to the crucial effect of other impurities (Ca, Cl, O, Pr etc) on the acid corrosion behaviour of Nd–base alloys.

3.2. *Atmospheric corrosion test*

The results of accelerated tests for the tested alloys of atmospheric corrosion in an 'industrial environment' containing 3 mg dm^{-3} SO_2 are shown in Fig. 2(a–c). As shown in Fig 2(a), the Fe additions (0.6–15%) do not influence the atmospheric corrosion rate; all the tested alloys corrode in this environment at practically the same rate as pure Nd (i.e. ~ 0.005 mg cm^{-2}h^{-1}). It should be noted that the Nd-base alloys clearly corrode slower than low carbon steel (~ 0.071 mg cm^{-2}h^{-1}– broken line in Fig. 2). Strictly speaking, the above mentioned value of the atmospheric corrosion rate for pure Nd was found after about 10 h of exposure. Its initial corrosion rate was 3–4 times greater. It seems that this long initial period is necessary for the production of an oxide layer which is thick and compact enough on the surface of pure Nd. The growth of the oxide layer is quickened by the presence of oxygen in the alloy. Recently Kim *et al.* [17] have shown that the presence of >0.6% oxygen in Nd–Fe–B type alloys strongly inhibits the atmospheric corrosion process.

The replacement of Nd with Tb in the Nd–Fe alloy has no effect on its atmospheric corrosion rate (Fig. 2(b)), however, the addition of 17% Dy is definitely unfavourable since it causes a strong increase in the oxidation rate after 20 h of exposure. Large additions of carbon into the Nd alloy are also disadvantageous (Fig. 2(c)). Small quantities of carbon ($\sim$0.1% C) do not accelerate the corrosion process, however, in the presence of 0.3% C the alloy corrodes three times faster and in the presence of 0.9% C even 5–10 times faster than pure neodymium.

The distinctly better resistance of the Nd-base alloys to atmospheric corrosion, when compared to carbon steel, suggests that oxide layers on the surface of Nd-base alloys have good isolating properties. Such properties disappear in the case of 17% Dy in the Nd-base alloy. It is also likely that greater quantities of carbon in the alloy can significantly worsen its atmospheric corrosion behaviour. A similar worsening of resistance to atmospheric corrosion of Nd–Fe–B type alloys for carbon concentrations greater than 0.2% C was lately found by Kim *et al.* [17].

3.3. *Polarization curves*

Because of the great electrochemical activity of rare earth metals the potentiokinetic measurements in strongly acid sulphate solutions (pH $\sim$ 0) showed very poor repeatability. On the other hand, large changes of pH at the tested electrode during fast potential scanning took place in neutral solutions.

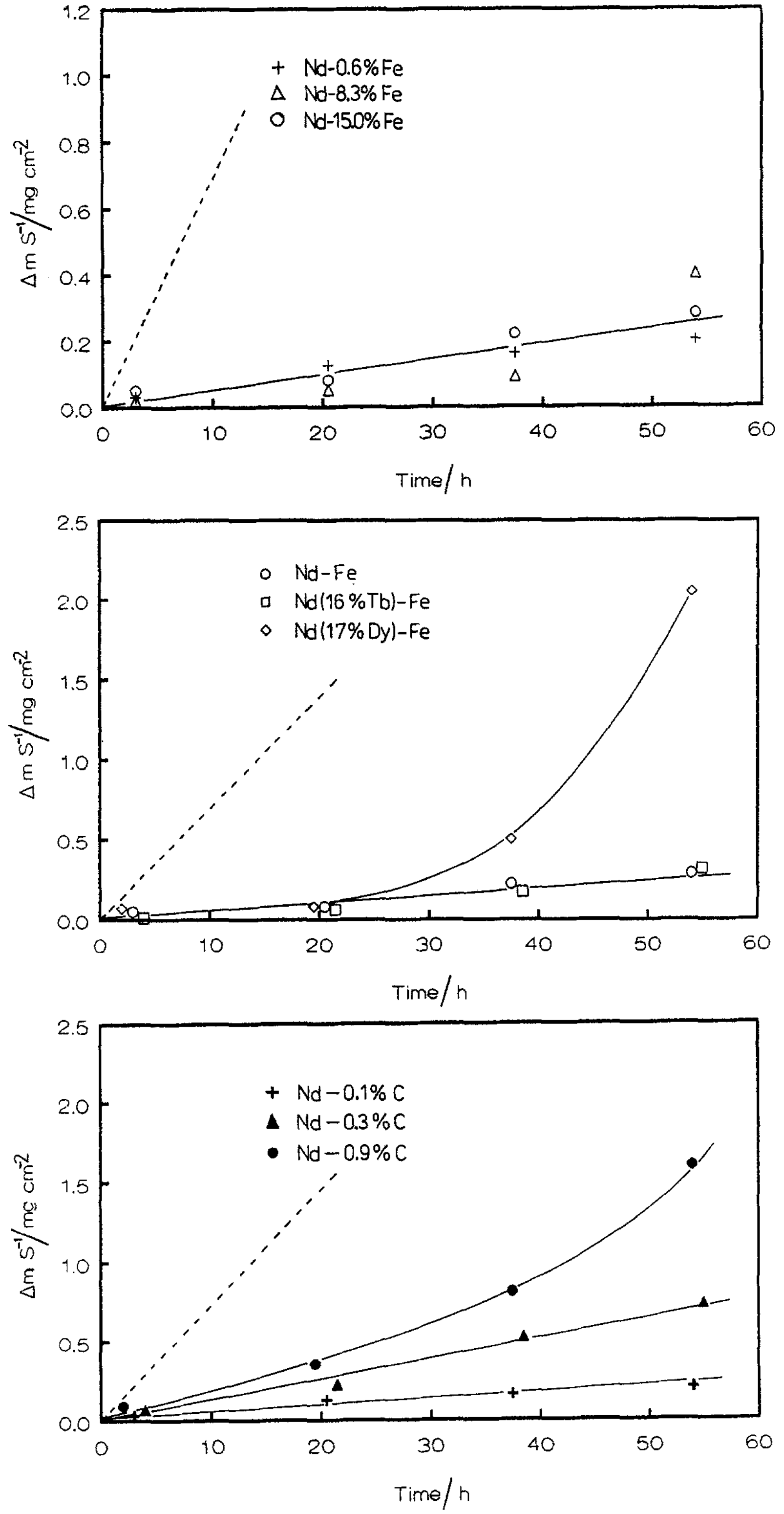

Fig. 2. Mass gain per cm^2 for three kinds of Nd-base alloys in humid air containing 3 mg dm^{-3} SO_2 (40° C). For comparison, broken lines show corrosion rate for low carbon steel.

A successful compromise is a test solution of 0.5 M $H_2SO_4 + 0.5$ M Na_2SO_4 with pH 3 for which the corresponding potentiokinetic polarization curves showed satisfactory reproducibility and pH changes were not detected during the experiment. However, the shape of polarization curves from such solutions depends on the length of time the electrode is immersed in the solution prior to the experiment. After immersing the electrode in the test solution, a series of 8–10 potentiokinetic curves were taken without changing the solution (time for completion of an individual curve was 15 s). For original curves, the cathodic currents were always much smaller and anodic currents much greater than for secondary curves. An example of such primary and secondary curves is presented in Fig. 3. The

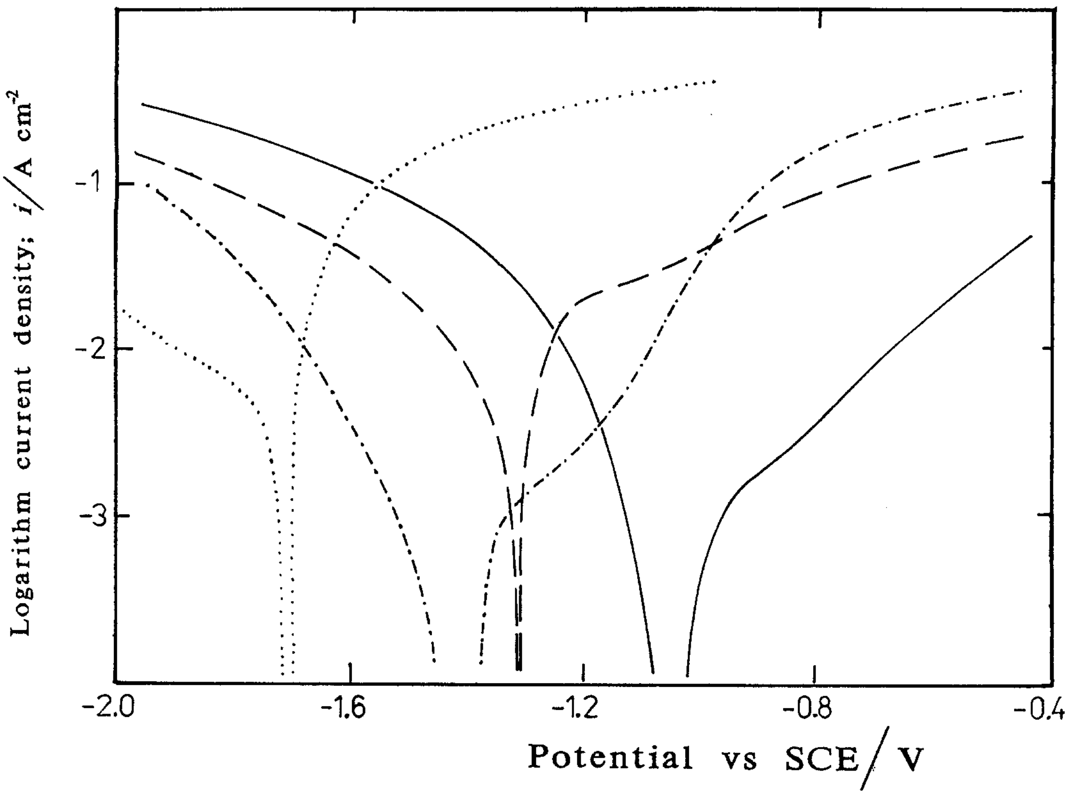

Fig. 3. Primary (I) and secondary (II) potentiokinetic polarization curves for pure Nd and Nd–15%Fe alloy in deaerated, 0.5 M sulphate solution with pH 3.0; 200 mV min^{-1}, 12 r.p.s., 25° C. Pure Nd: (I) ....., (II) — · — · —. Nd–15%Fe: (I) – – –, (II) ——.

same tendency was evident for all the alloys tested in this work. A possible reason for this 'hysteresis' for the potentiokinetic polarization curves is the enrichment of the surface by more noble elements. Both metallic (Fe) and non-metallic (C, carbides) products appear on the surface during the process of etching which results in development of the surface area for the cathodic process. In this way, for secondary curves, greater cathodic currents are observed (effect of surface development), whereas the decrease in the anodic currents is probably caused by the screening of the anodic surface by the enriched layers (slime). It seems however, that the hysteresis on the potentiokinetic polarization curves may also result from the generation of hydrides during cathodic exposure as the hysteresis is observed even for pure neodymium. The possibility of hydride production on the surface of cathodically treated Nd–Fe–B alloys has been considered in our earlier papers [18, 19]. On account of the good reproducibility of secondary polarization curves, only they are considered for further discussion. In Fig. 4 the primary and secondary curves for Nd–Fe alloys, and in Figs 5 and 6 secondary curves for Nd(Ln)–Fe and Nd–C alloys are presented. As can be seen from Figs 4–6, the polarization curves of all the investigated alloys exhibit only slight differences, but they clearly differ from the curve obtained for pure neodymium. Generally, the rate of hydrogen evolution on pure Nd is 10 to 100 times slower than on the tested Nd-base alloys (compare the relative movement of cathodic curves at a potential −1.6 V). On the other hand, the anodic dissolution rate for pure Nd is distinctly faster than for the alloys (compare anodic curves at a potential −0.8 V). Because there are no Tafel-segments on the polarization curves it is difficult to find the corrosion rates using extrapolation methods. Thus, the corrosion rates were evaluated by extrapolation of tangents to the cathodic lines with a slope of −0.12 V to the corrosion potential. This approximative method allows the evaluation of the corrosion rate with an accuracy of ±(30 to 40)%. Results of these calculations are presented in Table 3. Because of the high level of error in the i_{corr} values presented in Table 3 it is difficult to formulate unequivocal conclusions concerning the effects of alloying additions on the corrosion resistance of the tested alloys. However, it can be

Table 3. Corrosion potentials read from secondary potentiokinetic polarization curves and corrosion currents found by extrapolation of tangents to the cathodic curves to the corrosion potentials.

Sample	E_{corr} / V	i_{corr} / mA cm^{-2}
Nd–0.6Fe	−1.07	0.70 ± 0.20
Nd–8.3Fe	−1.11	0.90 ± 0.30
Nd–15 Fe	−1.05	0.40 ± 0.15
Nd–Fe	−1.05	0.40 ± 0.15
Nd(Tb)–Fe	−1.11	0.51 ± 0.20
Nd(Dy)–Fe	−1.13	0.98 ± 0.30
Nd–0.1C	−1.07	0.70 ± 0.30
Nd–0.3C	−1.15	0.40 ± 0.20
Nd–0.9C	−1.18	0.35 ± 0.10
pure Nd	−1.43	0.16 ± 0.05

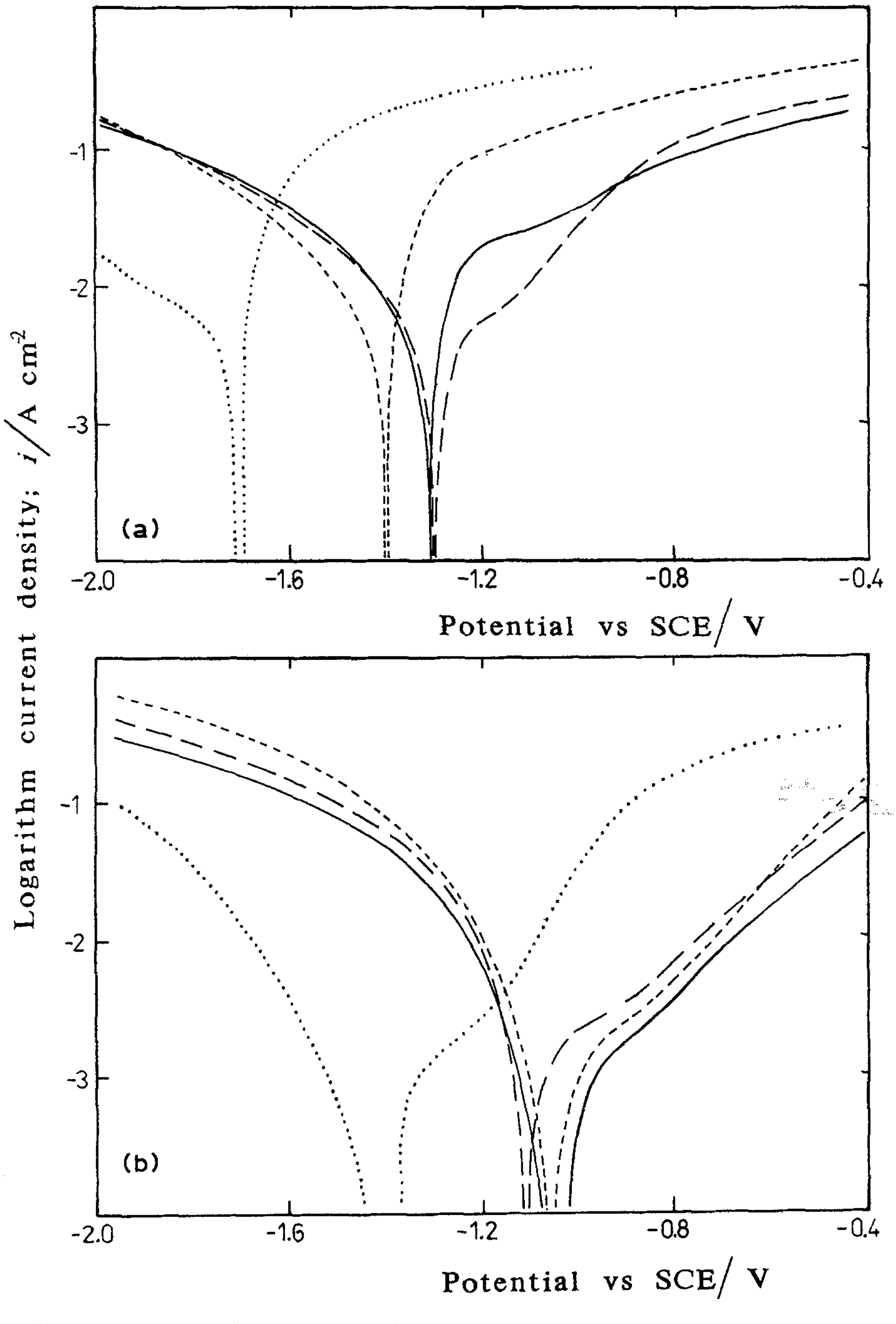

Fig. 4. Primary (a) and secondary (b) potentiokinetic polarization curves for the tested Nd–Fe alloys (pH 3, 200 mV min^{-1}, 12 r.p.s., 25° C. (......) Pure Nd; (- - -) Nd–0.6%Fe; (— — —) Nd–8.3%Fe; (———) Nd–15%Fe.

clearly seen that pure neodymium corrodes distinctly slower than the tested alloys. The alloying additions strongly accelerate the cathodic process of the reduction of hydrogen ions. The run of the potentiokinetic curves for Nd–Fe and Nd–C alloys in the anodic range confirms that the anodic process rate is inhibited by the generation of corrosion products on the surface.

4. Conclusions

(i) An acid corrosion process occurs faster for Nd-base alloys than for pure neodymium. The alloying additions (Fe,C) accelerate the cathodic reduction of hydrogen ions. At the same time, the anodic metal dissolution is inhibited by slime generated on the corroding surface.

(ii) Atmospheric corrosion for Nd-base alloys is distinctly slower than for carbon steel. Additions of carbon into the Nd worsen the atmospheric corrosion resistance of the alloy. Partial substitution of Nd by Dy is also disadvantageous for corrosion behaviour of the Nd–Fe alloy in an industrial atmospheric environment.

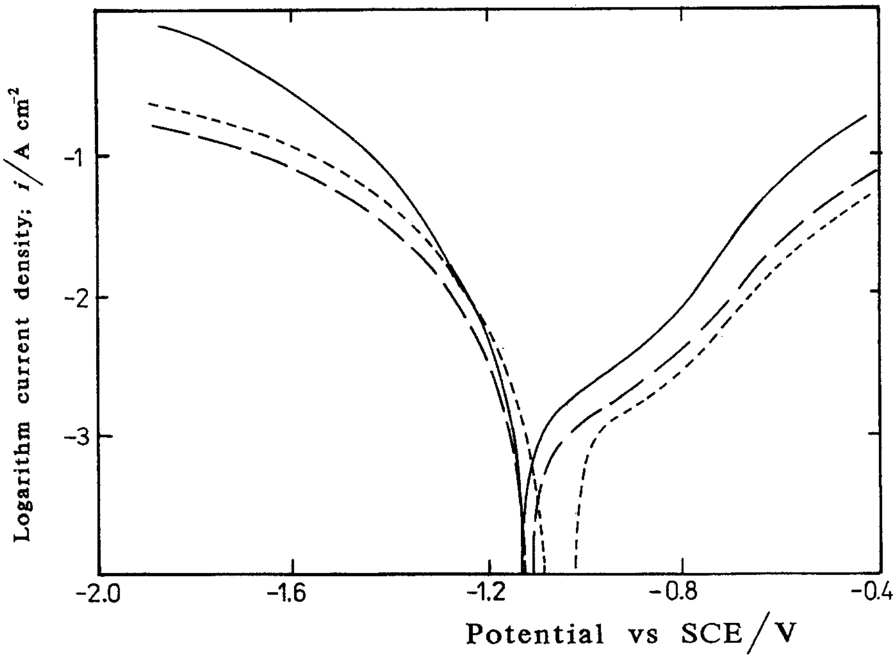

Fig. 5. Secondary potentiokinetic polarization curves for the tested Nd(Ln)–Fe alloys (pH 3, 200 mV min^{-1}, 12 r.p.s., 25° C). (- - - -) Nd–Fe; (– – –) Nd(Tb)–Fe; (——) Nd(Dy)–Fe.

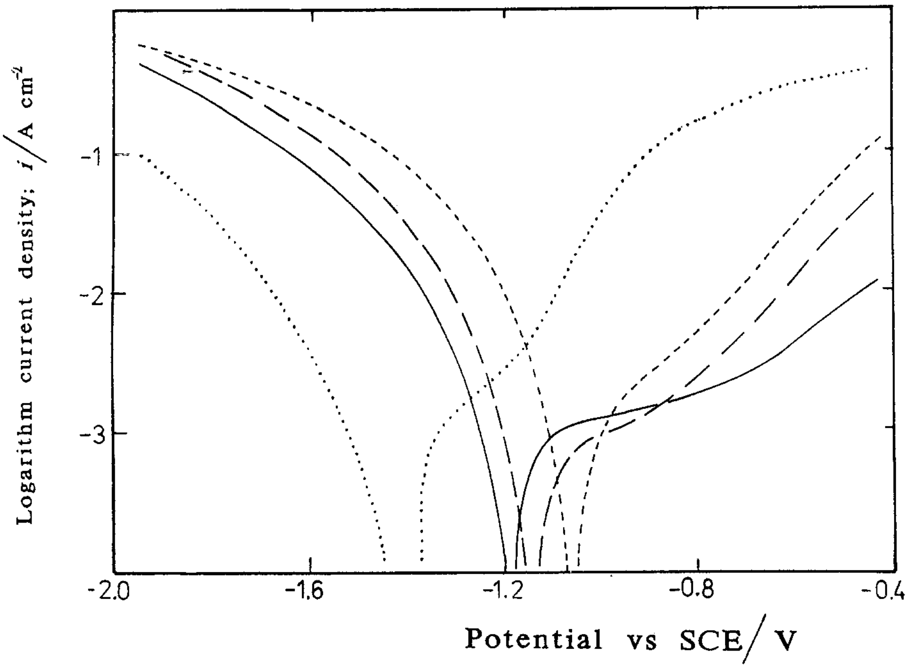

Fig. 6. Secondary potentiokinetic polarization curves for the tested Nd–C alloys (pH 3, 200 mV min^{-1}, 12 r.p.s., 25° C). (.......) Pure Nd; (- - - -) Nd–0.1%C; (– – –) Nd–0.3%C; (——) Nd–0.9%C.

References

[1] M. Pourbaix, 'Atlas of Electrochemical Equilibria in Aqueous Solutions', Pergamon Press, Cebelcor (1966).

[2] J. Jacobson and A. Kim, *J. Appl. Phys.* **61** (1987) 3763.

[3] H. C. Hua, G. Y. Wang, Q. Z. Xu, H. J. Jin and G. Q. Xu, *Phys. stat. sol. (a)* **125** (1991) 615.

[4] S. Szymura, H. Bala, G. Pawłowska, Yu. M. Rabinovich, V. V. Sergeev and D. V. Pokrovskii, *J. Less-Common Met.* **175** (1991) 185.

[5] H. Bala, S. Szymura and J. J. Wyslocki, *J. Mater. Sci.* **125** (1990) 571.

[6] H. Bala, G. Pawłowska, S. Szymura, V. V. Sergeev and Yu. M. Rabinovich, *J. Magn. Mater.* **87** (1990) 1255.

[7] H. Bala, S. Szymura, Yu. M. Rabinovich, V. V. Sergeev, G. Pawłowska and D. V. Pokrovskii, *Rev. Phys Appl.* **25** (1990) 1205.

[8] Yu. M. Rabinovich, A. V. Elutin, V. V. Sergeev and Yu. B. Patrikeyev, International Conference on 'The Outlook of Magnetic Materials in Eastern Europe', Berlin, 4–5, February (1991).

[9] T. Minowa, M. Shimao and M. Honshima, 35th Annual Conference on 3M, San Diego 29 October.–1 Nov. 1990, ref. No HA–08.

[10] N. D. Greene and F. G. Hodge, *Corrosion* **22** (1966) 206.

[11] L. Lee and N. D. Greene, *ibid* **20** (1964) 145t.

[12] B. N. Rybakov, A. F. Moskvicheva and G. D. Beregovaya, *Zashchita Met.* **9** (1973) 303.

[13] *Idem, ibid.* **10** (1974) 574.

[14] P. J. McGuiness, I. R. Harris, U. D. Scholtz and H. Nagel, *Z. Phys. Chem. N. F.* **163** (1989) 687.

[15] I. R. Harris, C. Noble and T. Bailey, *J. Less-Common Met.* **106** (1985) L1.

[16] K. Ohashi, Y. Tawara, T. Yokoyama and N. Kobayashi;

Proceedings of the 9th Workshop on Rare Earth magnets and their applications. Bad Soden, 31 Aug.–2 Sept. 1987, Deutsche Physikalische Gesellschaft e.V.; D–5340 Bad Honnef (1987) p. 355.

[17] A. S. Kim, F. E. Camp and E. J. Dulis, *IEEE Trans. Magn.* **26** (1990) 1936.

[18] H. Bala and S. Szymura, *Corros. Sci.* **32** (1991) 953.

[19] *Idem,* Proceedings of the 11th International Corrosion Congress, Vol. 5. 2–6 April 1990, Florence, Associazione Italiana cli Metallurgia, Milano, (1990), p. 5. 413.